J Polym Environ (2012) 20:932–943
DOI 10.1007/s10924-012-0488-4

ORIGINAL PAPER

Polylactide (PLA)—Halloysite Nanocomposites: Production, Morphology and Key-Properties

Marius Murariu · Anne-Laure Dechief · Yoann Paint · Sophie Peeterbroeck · Leila Bonnaud · Philippe Dubois

Published online: 29 June 2012

Abstract To evaluate the potential of halloysite nanotubes (HNT) as nanofiller for polylactide (PLA), various nanocomposites have been successfully produced by melt-blending the polyester matrix with HNT (HNT(QM)). HNT were also surface treated by silanization reaction with 3-(Trimethoxysilyl) propyl methacrylate (TMSPM). The morphology, thermal, tensile and impact strength properties of the nanocomposites containing 3–12 % HNT were evaluated and compared to those of pristine (unfilled) PLA. The nanocomposites were characterized by higher rigidity (with Young's modulus increasing with HNT loading), higher tensile strength (about 70 MPa at 6 % HNT(QM)), whereas the elongation at break and impact strength did not decrease. As demonstrated under dynamic solicitation (DMA), melt-blending PLA with HNT led to enhancement of storage modulus (E′) and offers the possibility to use PLA in applications requiring higher temperatures of utilization. However, with few exceptions, TGA and DSC measurements did not reveal important changes of thermal parameters. The surface silanization treatment proved to improve the quality of the nanofiller dispersion even at higher loading. As a result, good thermal stability associated to high tensile strength, and noticeable increases in impact properties were recorded. Furthermore, enhanced nucleating ability and crystallization kinetics of the PLA matrix were revealed as specific characteristics.

Keywords Polylactide · Halloysite nanotubes · Nanocomposites · Impact strength

M. Murariu (✉) · A.-L. Dechief · Y. Paint · S. Peeterbroeck · L. Bonnaud · P. Dubois (✉)
Center of Innovation and Research in Materials and Polymers (CIRMAP), Laboratory of Polymeric and Composite Materials (LPCM), University of Mons and Materia Nova Research Center, Place du Parc 20, 7000 Mons, Belgium
e-mail: marius.murariu@materianova.be

P. Dubois
e-mail: philippe.dubois@umons.ac.be

Introduction

Polylactide or polylactic acid (PLA) is currently receiving considerable attention for conventional utilization such as packaging materials as well as production of fibres, and more recently, as (nano)composites for technical applications. In competition with petroleum-based polymers and showing a principal position on the market of bio-based polymers, PLA is undoubtedly one of the most promising candidates for further developments owing of its additional biodegradability [1–6].

Furthermore, very recent trends highlight the huge potential of PLA-based products with higher added value for engineering applications, i.e., in transportation, electronic and electrical devices, mechanical and automotive parts, etc. Consequently and to reach the end-user demands, the profile of PLA properties can be tuned up by combining PLA with different dispersed phases: micro- and nano-fillers, flame retardants, impact modifiers, plasticizers and other additives [3, 4, 7–15].

Polymer nanocomposites (PNC) with improved properties (stiffness, thermal stability, fire retardancy (FR), antistatic to conductive electrical characteristics, lower permeability, crystallization enhancement, anti-UV and antibacterial action, etc.) have been produced by combining PLA with various nanofillers such as organo-modified

layered silicates (OMLS), carbon nanotubes (CNT), graphite derivatives, polyhedral oligomeric silsesquioxanes (POSS), zinc oxide, etc. [7, 8, 16–24].

Halloysite nanotubes (HNT) have recently received considerable attention as a new type of nanofiller for enhancing the mechanical, thermal, crystallization, fire and other specific properties of different polymers like PA6, PA12, PP, PS and epoxy resins, etc. [25–34].

As reported elsewhere [25–27, 31], the composition of HNT is similar to kaolin, whereas taking into account the state of hydration, the ideal chemical formula can be expressed as $Al_2Si_2O_5(OH)_4 \times nH_2O$, where n (representing the hydrated and dehydrated forms) equals 2 and 0, respectively for HNT and kaolin. The tubular structure of HNT is believed to be the result of hydrothermal alteration or surface weathering of aluminosilicate minerals. Due to several characteristic features such as nanoscale lumen, relatively high length-to-diameter ratio, and low hydroxyl group density on their surface, HNT are considered as promising competitors and cheaper alternatives to both CNT and OMLS. Conventional nanoclays require exfoliation to separate the layers and to obtain the adequate dispersion needed for uniform properties in PNC whereas HNT do not require exfoliation, making possible the production of stronger, lighter materials without the complexity and processing cost associated with intercalation and exfoliation [34, 35].

Unfortunately and compared to the extensive evaluation of OMLS and CNT as nanofillers for PLA, investigations on PLA/HNT nanocomposites appear to be missing or have not been conducted so far to evidence the overall effect of HNT addition on main PLA properties. In our opinion, the interest for HNT is rather new, and more likely represents the main reason explaining the lack of studies concerning the production and characterization of PLA-HNT nanocomposites. Generally, the addition of nanofillers can provide PLA with relevant specific properties but sometimes also triggers problems such as loss of mechanical and thermal characteristics, degradation of this water-sensitive polyester matrix, which are important aspects to be considered when targeting a potential application.

In response to the demand for new PLA grades characterized by improved characteristic features, HNT were evaluated as potential new nanofiller for PLA. Commercially available HNT (or additionally silane treated) were added into a PLA matrix (extrusion grade) via melt-compounding technology and the resulting nanocomposites were characterized in detail for highlighting their performances. Surface treatment of HNT was also studied via silanization reaction in order to improve the nanofiller dispersion within PLA.

Experimental

Materials

Poly(L,L-lactide)—hereafter called PLA, was kindly supplied by NatureWorks LLC. Characteristics of PLA are as follows: number average molecular weight, $M_{n(PLA)} = 88{,}500$, index of polydispersity, $M_w/M_n = 1.8$, D isomer content <2 %.

Halloysite nanotubes (referred below as "HNT") were kindly supplied by NaturalNano, Inc. (USA) as HNT(QM) (HNT milled and treated). Following the information presented elsewhere [36, 37], the organic modifier used to surface-treat these HNT(QM) is a quaternary ammonium chloride salt [31], in amount less than 5 % according to the technical sheet of the product [38].

A selected silane, i.e., 3-(Trimethoxysilyl) propyl methacrylate (98 %), supplier Acros Organics (called below TMSPM), was used for the additional treatment of the nanofiller. The silane-treated nanofiller will be reported as HNT(s).

Production of PLA Nanocomposites

Before processing by melt-blending, PLA was dried overnight at 80 °C under vacuum. To minimize the water content for melt-blending with PLA, the nanofiller was dried at 105 °C for 48 h and then used directly for melt-compounding. The nanofiller was mixed together with PLA at 200 °C under moderate mixing (cam blades) by using a Brabender bench scale kneader (50EHT model) following a specific procedure: 3 min premixing at 30 rpm- speed in order to avoid an excessive increase of the torque during melting of PLA, followed by 7 min mixing at 70 rpm. For the sake of comparison, pristine PLA was processed under similar conditions of melt-compounding. Throughout this report, all percentages are given as wt %.

In a second step, PLA-HNT(s) nanocomposites containing up to 12 % HNT(s) were obtained after the previous treatment of the nanofiller (HNT(QM)) with a selected silane (TMSPM). Firstly, HNT were treated with 3 % silane (from a solution of 1 % TMSPM in methanol/demineralized water (9/1)) following the slurry method reported by Sadler and Vecere [39]. The chemical treatment of the nanofiller surface was followed by evaporation of the solvents (i.e., water and alcohol) and finally drying under vacuum at 80 °C.

Plates (~3 mm thick) for mechanical characterizations were produced by compression molding at 190 °C by using an Agila PE20 hydraulic press. More specifically, the material was first pressed at low pressure for 240 s (3 degassing cycles), followed by a high-pressure cycle at 150 bars for 150 s. The resulted samples were then cooled

under pressure (50 bars). Specimens for tensile and Izod impact tests were obtained from plates by using a milling-machine in accordance with ASTM D 638-02a (specimens type V) and ASTM D 256-A norm (specimens 60 × 10 × ~3 mm^3), respectively.

Characterization

Thermogravimetric Analyses (TGA)

TGA were performed by using a TGA Q50 (TA Instruments) with a heating ramp of 20 °C/min under air flow, from room temperature up to 600 °C (platinum pan, 60 cm^3/min air flow rate).

Differential Scanning Calorimetry (DSC)

DSC measurements were performed by using a DSC Q200 from TA Instruments under nitrogen flow. The samples obtained by compression molding were investigated. The procedure was as follows: first heating scan at 10 °C/min from 0 up to 200 °C, isotherm at this temperature for 2 min, then cooling down to −20 °C at 10 °C/min and finally, second heating scan from −20 to 200 °C at 10 °C/min. The first scan was meant to erase the anterior thermal history of the samples. The events of interest, i.e., the glass transition temperature (T_g), cold crystallization temperature (T_c), enthalpy of cold crystallization (ΔH_c), temperature and enthalpy of polymer chain rearrangement (T_r and ΔH_r, respectively), melting temperature (T_m) and melting enthalpy (ΔH_m) were evaluated. The degree of crystallinity (χ_c) was determined by subtracting ΔH_c and ΔH_r (if it was evidenced) from ΔH_m, and by considering a melting enthalpy of 93 J/g for 100 % crystalline PLA.

Screening analyses to have information about the effect of HNT addition on the crystallization kinetics of PLA were performed through determination of crystallization half-time ($t_{1/2}$) during isothermal crystallization. Using DSC, the PLA samples were heated to 200 °C at a rate of 10 °C/min, held 2 min at this temperature to erase their thermal history, step followed by high speed-cooling (rate of about 40 °C/min) to the iso-crystallization temperature of interest (110 or 120 °C) and maintained under isothermal conditions for up to 60 min.

Mechanical Testing Measurements

Tensile testing measurements were performed by using a Lloyd LR 10 K tensile bench in accordance to the ASTM D 638-02a norm at a speed rate of 1 mm/min using a distance of 25.4 mm between grips. Notched impact strength (Izod) measurements were performed by using a Ray-Ran 2500 pendulum impact tester and a Ray-Ran 1900 notching apparatus, in accordance to the ASTM D 256 norm (method A, 3.46 m/s impact speed, 0.668 kg hammer).

All mechanical tests were carried out by using specimens previously conditioned for at least 48 h at 20 ± 2 °C under a relative humidity of 50 ± 3 % and the values were averaged out over five measurements.

Dynamic Mechanical Analysis (DMA)

DMA on selected samples (specimens of 60 × 12 × 2 mm^3 performed by injection molding at 200 °C, DSM micro-injection molding machine) were carried out using DMA 2980 apparatus (TA Instruments) in a dual-cantilever bending mode. To avoid a different thermal history after the processing by injection molding or an additional crystallization process during testing, the specimens were annealed under similar conditions (at 110 °C under vacuum for 90 min). The dynamic storage and loss moduli (E′ and E″, respectively) were determined at a constant frequency of 1 Hz as a function of temperature from 0 to 120 °C, at a heating rate of 3 °C/min.

Transmission Electron Microscopy (TEM)

Transmission electron micrographs of PLA/HNT nanocomposites were obtained with a Philips CM200 apparatus using an accelerator voltage of up to 120 kV. The nanocomposite samples (70–80 nm thick) were prepared with a Leica Ultracut UCT ultracryomicrotome by cutting at −100 °C. Reported microphotographs represent typical morphologies as observed at, at least, three different locations of the sample.

Results and Discussion

HNT as Nanofiller for PLA

Firstly, it is worth mentioning that HNT from different sources can vary in the level of hydration, morphology (dimension of inner and outer diameter, length, length-to-diameter ratio) and colour, depending on the substitutional metals and on mineral origin [25, 30, 31]. However, TEM images at different magnifications (Fig. 1a, b) of as received HNT(QM) assess the tubular morphology of HNT (outer tube diameter of 50–60 nm and lumen size of 20–30 nm, Fig. 1b) as well as the presence of nanotubes of diverse length, ranging typically from hundreds of nanometres to above 1.5 μm. Noteworthy, the presence of nanotubes of various lengths in the TEM images (Fig. 1a) is mainly ascribed by us to the milling process performed

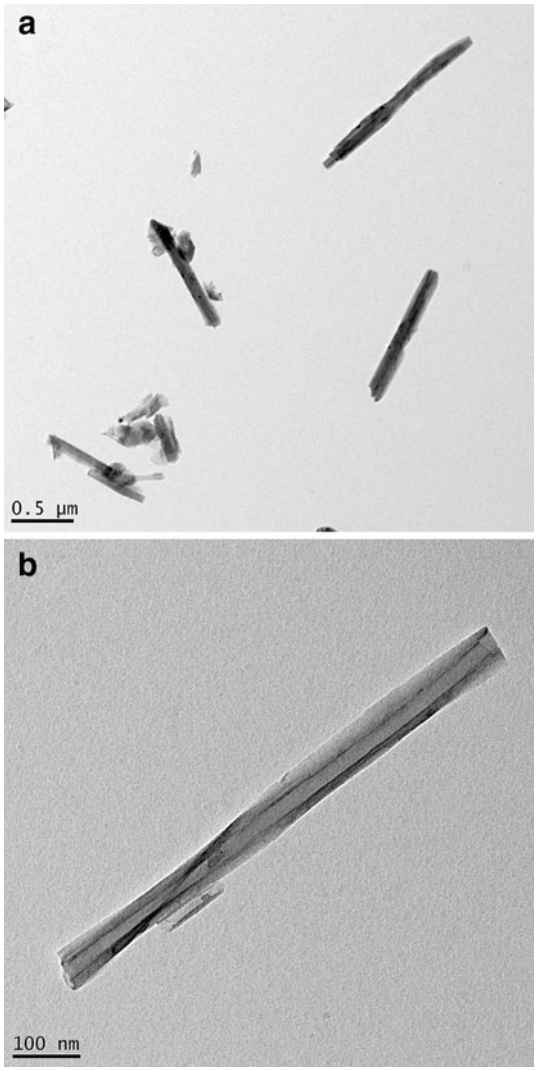

Fig. 1 **a**, **b** TEM images at different magnifications of as received nanotubes (HNT(QM))

by the industrial supplier, which can affect, more or less, the length-to-diameter ratio of HNT.

On the other hand, in the perspective of PNC preparation, it is worth recalling that PLA is very sensitive to hydrolysis, temperature, shear, etc. during melt-processing, so all precautions known in the state of the art should be applied to limit polyester chains degradation.

From TGA of as received HNT(QM) (Fig. 2) it comes out that the weight loss during thermal heating (20 °C/min) of the as received nanofiller occurs in three distinguishable regions:

1. Below 100 °C, indicating the presence of absorbed free water (about 1.3 %).

This water will be removed by drying before mixing with PLA, but further precaution it is required to avoid the contact of the nanofiller with the atmospheric moisture.

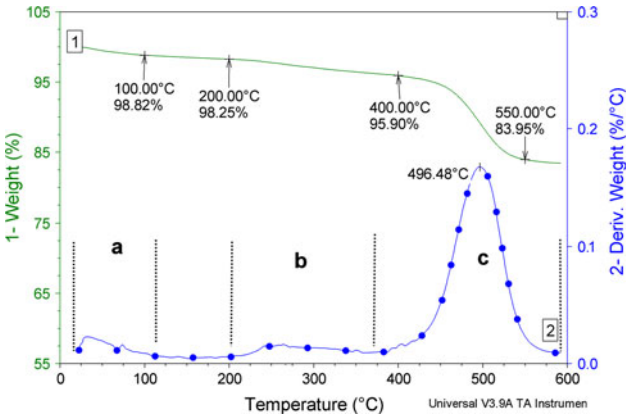

Fig. 2 TGA of as received HNT(QM) (under air, 20 °C/min)

2. A weight loss of ~2.4 % in the interval of temperature between 200 and 400 °C (d-TG shows a maximum above 260 °C), ascribed to the loss of hydration water molecules that can be present between the layers of HNT and to degradation of the organomodifier product.

Based on the different sources of information, i.e., publications and patents, it is reported that the HNT can be surface treated with quaternary ammonium chloride salts [31, 37, 38]. However, from TGA results it comes out that the nanofiller is containing a relatively low amount of hydrated water (a previously drying process carried out by the supplier is assumed), whereas the dispersing agent used as organomodifier is in evident lower amount by comparing to the commercial OMLS that are often modified with 20–40 % quaternary ammonium salts [7, 8, 40].

3. Dehydroxylation at higher temperature than 400 °C (weight loss above 12 %, with a maximum on d-TG curve at about 497 °C).

Furthermore, these data are consistent with the mechanisms and results of different studies reported elsewhere connected to HNT and their utilization [26, 34, 41].

To minimize PLA degradation by hydrolysis, the nanofiller was dried at 105 °C for 48 h. Besides, it was presumed by us that a higher temperature of drying, e.g., 200 °C, could lead to thermal degradation of the organomodifier of HNT(QM), as reported in the case of OMLS [40].

As far as the additional treatment by silanization is concerned, various silane agents have been reported for modifying the surface of HNT: γ-methacryloxypropyltrimethoxysilane [29], aminoethylaminopropyltrimethoxysilane [34], γ-aminopropyltriethoxysilane [42].

HNT contain two types of hydroxyl groups, inner and outer hydroxyl groups, which are located between the layers and on the surface of the nanotubes, respectively

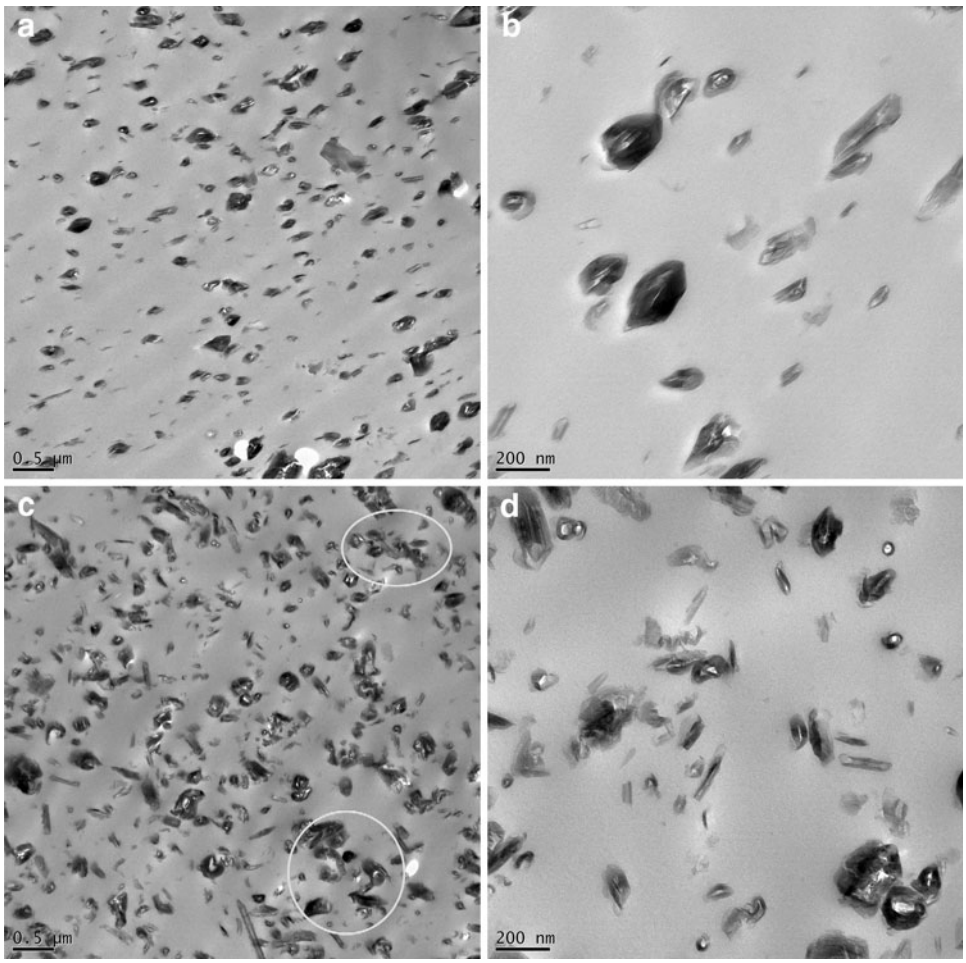

Fig. 3 **a–d** TEM pictures at different magnifications of PLA-HNT(QM) nanocomposites containing 6 % (**a, b**) and 12 % (**c, d**) halloysite nanotubes

[25]. Following the chemical mechanism of silanization, hydrolysis of the alkoxy groups into silanols first occurs, which can react with the hydroxyl groups of the inorganic HNT and eliminate water. Furthermore, it is assumed that Si–O–Si layers can be formed by reaction of silane molecules with each other to give a multimolecular structure of bound silane coupling agents [43] on the surface of filler (here, HNT) that will behave as interfacial zone, effectively playing a compatibilizing role. Accordingly, in our experiments, the HNT were additionally treated with 3 % silane agents functionalized with a methacryloxy moiety, i.e., TMSPM, which proved high efficiency in terms of HNT(s) dispersion in PLA (vide infra).

Properties of PLA-HNT(QM) Nanocomposites

Morphology

Information concerning the morphology of nanocomposites was mainly obtained through TEM analyses. Figure 3a, b and c, d show selected pictures of the nanocomposites produced by addition into PLA of 6 and 12 % HNT(QM), respectively. It is obvious from the TEM images recorded at lower magnification (Fig. 3a, c) that a good quality of the distribution/dispersion of the HNT(QM) is reached throughout the polyester matrix even though the melt-mixing was performed under moderate shear (internal kneader). However, some small aggregates (identified by white circles in Fig. 3c) were evidenced in the TEM pictures containing the higher amount of HNT(QM), i.e., 12 % HNT.

Besides, the TEM images at higher magnification (Fig. 3b, d) attest for the good dispersion of HNT(QM) through PLA where quite well-individualized nanotubes are typically observed. This may be explained as in the case of PP-HNT(QM) nanocomposites [31] by the presence of the organomodifier at the nanotube surface, which decreases the surface free energy and nanotube/nanotube interactions, thereby breaking up the formation of aggregates during the melt-blending process.

Following the TEM observations, HNT(QM) thus appear easily dispersible into PLA, and as reported elsewhere [25, 31], the limited intertubular contact area and rod-like geometry, associated with the surface treatment,

Table 1 TGA data of pristine PLA and PLA-HNT(QM) nanocomposites (under air flow, 20 °C/min)

Entry	Sample (%, by weight)	Temperature for 5 % weight loss, °C	Temperature of the max. rate of degradation, °C (from d-TG)	Residue (%)
1	PLA (processed)	330	377	0.2
2	PLA- 6 % HNT(QM)	330	373	5.0
3	PLA- 12 % HNT(QM)	332	372	10.3

can be considered as key-factors that explain their good dispersion. In the same context, it is also worth mentioning that a good dispersion of HNT was also identified in some other polar polymers such as PA6 or PA12 [25, 44].

Thermal Properties

To highlight the effect of HNT(QM) on PLA thermal stability, TG measurements performed on the nanocomposites have been compared to those of pristine PLA. For simplification and easier interpretation, Table 1 summarizes the values of the temperature for 5 % weight loss ($T_{5\%}$) and of the temperatures corresponding to the maximum rate of thermal degradation (T_D—from d-TG). It is of interest to note that $T_{5\%}$ is often considered as the initial decomposition temperature. From the data presented in Table 1, it comes out that the nanocomposites show comparable thermal stability ($T_{5\%}$ as parameter) and only a slight decrease in T_D is recorded with respect to the processed unfilled PLA. The decrease of T_D at higher loading of nanotubes is mainly assigned to the residual water of hydration and to the degradation of ammonium organo-modifier (see "HNT as Nanofiller for PLA" section), without totally excluding some additional effect of metallic impurities naturally contained in clays, which can also trigger faster degradation of the polyester matrix. Additionally, as suggested in previous studies, since HNT display lower aspect ratio and specific surface area than most of the OMLS, it is reasonable to assume that the barrier effect of HNT with tubular structure may somewhat be inferior to those of layered silicates [29, 44].

Figure 4 shows representative DSC curves recorded during the second heating scan of PLA-HNT(QM) nanocomposites compared to those of pristine PLA. Firstly, from these data it comes out that the addition of nanofiller does not modify significantly the T_g values, which remain in the range 61–63 °C, and T_m values of PLA matrix ($T_m \approx$ 163–170 °C). The multiple T_m peaks or presence of shoulders on DSC curves, can be ascribed to the melting of crystalline regions of various size and perfection formed during cooling and crystallization processes, without excluding the influence of additional factors that can affect

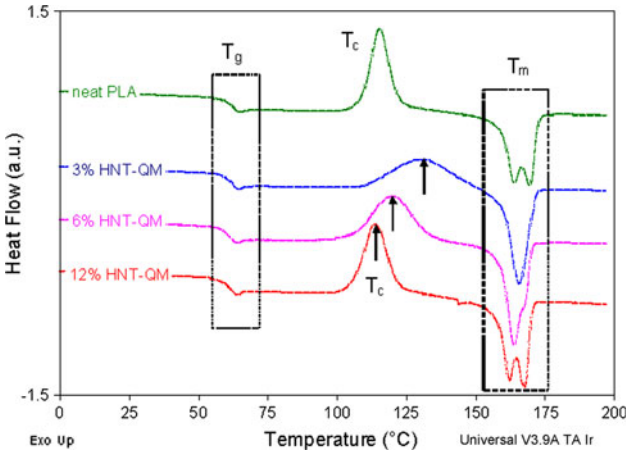

Fig. 4 DSC traces obtained during second heating scan (10 °C/min) of PLA and PLA-HNT(QM) nanocomposites

the melting of PLA (different crystalline structures, presence of fractions of low molecular weight, the chemical treatment and nanofiller loading, the effect of thermo-mechanical processing and time–temperature history, etc.) [7]. However, the recrystallization and the melting can be competitive in the heating process, whereas the double-melting behaviour is attributed to the slow rates of PLA crystallization and recrystallization [45]. Furthermore, the lower temperature peak is generally associated to the melting of the small crystals produced by the secondary crystallization, and the peak recorded at higher temperature, to the melting of the major crystals formed in the primary crystallization process [46].

DSC also reveals that the polymer matrix undergoes cold crystallization, while T_c in nanocomposites decreases in correlation with the percentage of HNT. Furthermore, there is no clear changes of χ_c recorded in non-isothermal crystallization (rate of cooling of 10 °C/min) meaning that HNT(QM) do not seem to behave as efficient nucleating agents of PLA crystallization like in the case of other PNC containing the same nanofiller [25, 30, 31, 44]. However, it is assumed that due to a relatively high cooling rate (10 °C/min) for a polymer characterized by low crystallization ability, the χ_c of PLA in nanocomposites is remaining

limited, to values in the range of 3–4 %, somewhat comparable to those recorded for the pristine PLA (2.7 %).

Thermo-Mechanical Properties

In general, addition of nanofillers into a polymer matrix is expected to result in improved properties, such as better tensile and flexural strength, higher modulus, dimensional stability, higher heat distortion temperature, etc. According to previous investigations, by adding HNT in different polymers (PA6, PA12, PBT, PP, etc.) the flexural strength, modulus, tensile and impact strength can be improved [25, 27, 28, 31, 44]. The reinforcing effect of HNT on different polymers, frequently observed at low loadings, is generally ascribed to the rod-like and high aspect ratio structure, whereas their interfacial properties can play a key-role as well.

Figure 5 shows the evolution of both tensile strength and rigidity (Young's modulus) of the nanocomposites in function of the nanofiller content. Comparison to pristine PLA is also given. On one hand, by comparison to neat PLA, both rigidity and stress (given as maximum tensile strength) are gradually improved in nanocomposites by increasing the percentage of nanofiller up to 6 %. However, at higher loading, the rigidity is maintained at high level while no further increase in tensile strength is observed. Such an observation is generally attributed to somewhat inevitable aggregation of the nanofiller at higher loading. In fact this assumption was obviously confirmed by additional experiments to assess the production of PLA composites filled with 20–30 % HNT(QM), which revealed a dramatic decrease in tensile strength (results not discussed here).

The PLA nanocomposites containing up to 12 % HNT(QM) revealed similar nominal strain at break (ε_b) as the pristine polyester matrix (values of about 5 %), whereas the Izod impact strength (see Fig. 9) is not decreased, with values comparable to neat PLA (2.8 kJ/m^2), at least for the investigated contents in nanofiller (from 3 to 12 %). By comparing to other nanofillers that lead to PLA nanocomposites with improved rigidity, mostly in the detriment of the decrease of ε_b and impact strength (e.g., expanded graphite [21]), this behaviour is quite remarkable and is commonly ascribed to the intrinsic stiffness of the nanotubes- resulting from their tubular structure, their good dispersion, as well as to the good interfacial properties between filler and matrix [25, 27, 28, 44]. The excellent tensile strength (about 70 MPa for a nanocomposite containing 6 % HNT(QM)), corroborated with the increase of rigidity and good level of impact properties, suggests that the PLA-HNT composites can be potentially interesting in engineering applications.

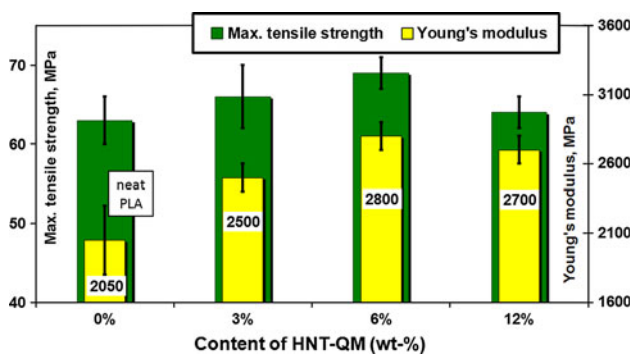

Fig. 5 Evolution of tensile strength and Young's modulus of PLA and PLA–HNT(QM) nanocomposites with different content of nanofiller

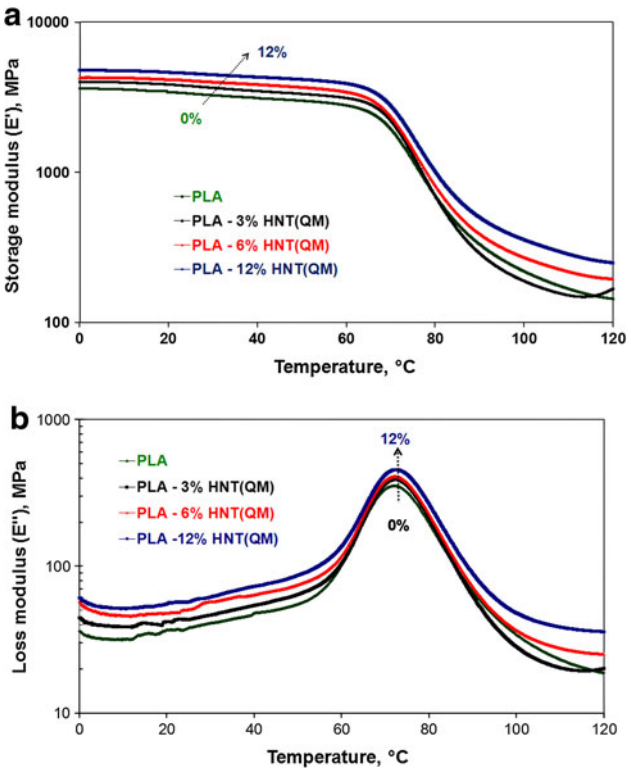

Fig. 6 **a**, **b** Dependencies of E′ **a** and E″ **b** versus temperature: pristine PLA with respect to PLA-HNT(QM) nanocomposites

Figure 6a, b show the temperature dependencies of storage (E′) and loss (E″) moduli of pristine PLA and nanocomposites obtained by addition of 3–12 % HNT(QM). For the sake of clarity, only one representative curve as the average of minimum two measurements is shown for each sample.

At low temperature the values of E′ decreased gradually in a similar way (Fig. 6a) for all the samples. However, in correlation to nanofiller content, E′ increases distinctly for the nanocomposite samples, e.g., at 20 °C the value of E′ is 3,400 MPa for neat PLA, 4,100 and 4,600 MPa for PLA containing 6 and 12 %, HNT(QM), respectively. In

Table 2 Comparative DMA data of PLA and PLA nanocomposites containing HNT(QM) and HNT(s)

Type of nanofiller → Parameter → Wt., % ↓	HNT(QM)		HNT(s)	
	E′ value at 50 °C (MPa)	Temperature for a value of 3,000 MPa (°C)	E′ value at 50 °C (MPa)	Temperature for a value of 3,000 MPa (°C)
0	3,000	50.2	3,000	50.2
3	3,300	63.1	3,100	54.8
6	3,700	65.9	3,800	66.3
12	4,100	68.9	3,600	65.4

addition, in relation to the potential interest for the utilization of these nanocomposites in mechanical applications and at higher temperature, it is worth mentioning that the value of E′ of 3,000 MPa is obtained at 50.2 °C for pristine PLA with respect to 65.9 and 68.9 °C for nanocomposites with 6 and 12 % HNT(QM), respectively (Table 2).

DMA was also used for investigation of the loss modulus (E″) as function of temperature (Fig. 6b).

The increase of E″ with the filler content can be attributed mainly to the contribution of the mechanical loss generated at the interface regions between nanotubes and PLA matrix [47]. However, in agreement with the DSC results, the data reveal that there are no significant differences between the temperatures corresponding to the maximum of E″ (~73 °C) of PLA and those of PLA-HNT(QM) nanocomposites. Furthermore, it should be also noted that DMA results from the viscoelastic behaviour are correlated with the mechanical properties, suggesting the reinforcing effect of nanofiller. Additionally, the reinforcement factor calculated following the procedure reported elsewhere [48] is improved by addition of nanofiller, noteworthy not only in the glassy state, but also above the T_g of PLA.

As preliminary conclusion, interesting mechanical properties have been recorded at relatively low amount of nanofiller (3–6 % HNT(QM)), which can be ascribed to the reinforcing effect of the halloysite nanotubes that proved to be finely distributed and dispersed within the PLA matrix, at least at relative content up to 6 %. As demonstrated by DMA (dynamic solicitation), melt-blending PLA with HNT leads to the enhancement of the storage modulus (E′) and offers the possibility to use PLA in applications requiring rigidity at higher temperatures of utilization.

PLA-HNT(s) Nanocomposites

In order to further increase the dispersion ability of the inorganic nanotubes in PLA and increase the affinity between the dispersed HNT and the polyester chains, additional treatment of HNT(QM) with silane (TMSPM) has been performed (see experimental). The so-prepared silanized halloysite nanotubes, coined as HNT(s), were then dispersed in PLA by melt-processing for producing PLA nanocomposites containing up to 12 % HNT(s). The main objective of this section is to discuss the most important aspects that can be associated to the effectiveness of silane treatment and to the key-performances of the related PLA-HNT(s) nanocomposites.

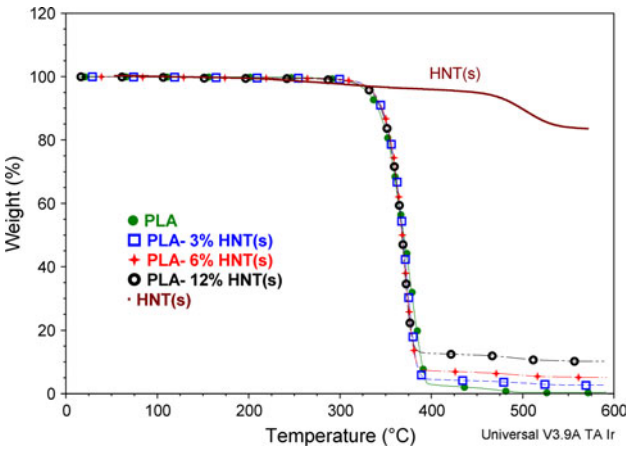

Fig. 7 TGA of HNT(s), PLA and PLA-HNT(s) nanocomposites (under air, 20 °C/min)

Thermal Properties and Crystallinity

First of all, Fig. 7 shows the comparative TG curves of HNT(s), those of PLA and the corresponding nanocomposites. On one hand, HNT(s) are characterized by a weight lost above 16 % up to a temperature of 550 °C, whereas the maximum on d-TG curve is slightly shifted to 504 °C. On the other hand, the addition of HNT(s) into PLA is leading once more to nanocomposites characterized by good thermal stability ($T_{5\%}$ in the range 334–337 °C, T_D above 370 °C) quite similar with the neat PLA.

Moreover, the second DSC heating scan (non-isothermal crystallization, after previously cooling with a rate of 10 °C/min) of PLA-HNT(s) samples did not attest significant modifications (increases of χ_c, changes of T_g or T_m,

Table 3 Comparative DSC data (first heating, 10 °C/min) of PLA and PLA nanocomposites containing HNT(QM) and HNT(s) (samples after the compression molding process)

Type and nanofiller content (%, by weight)	T_c/T_r (°C)	$\Delta H_c/\Delta H_r$ (J g^{-1})	T_m (°C)	ΔH_m (J g^{-1})	χ_c (%)
PLA	110	25.0	170	34.5	10.2
3 % HNT(QM)	97/152	20.1/1.7	167	35.8	15.1
6 % HNT(QM)	118	30.3	163; 168	35.9	6.0
12 % HNT(QM)	110	30.3	162; 168	36.4	6.6
3 % HNT(s)	96/155	11.5/0.7	172	27.4	16.3
6 % HNT(s)	90/152	14.3/1.4	168	37.8	23.8
12 % HNT(s)	91/155	12.1/1.0	173	30.8	19.0

etc.- results not shown here), with respect to the pristine PLA and PNCs containing HNT(QM). Interestingly enough, the most important differences concern the values of χ_c as they are revealed by the first DSC heating scan, which typically assesses the thermal characteristics of the specimens used for mechanical testing. For illustration (Table 3), the PNC filled with 3–12 % HNT(s) are typically characterized after the compression molding process by a higher χ_c, i.e., values in the range 16–24 % by comparing to less than 15 % in the case of nanocomposites containing similar loadings of HNT(QM), or to pristine PLA, that practically shows a χ_c of about 10 %.

It is important to remind that the use of PLA in technical applications (e.g., injection molded products) remains limited because PLA is known for a relatively too slow crystallization rate when it is compared with many other semi-crystalline thermoplastics. A measure of the effectiveness of different nanofillers as nucleating agents is the crystallization half-time ($t_{1/2}$) as recorded in isothermal crystallization experiments. The effects of HNT(s) with respect to HNT(QM) on the crystallization kinetics of PLA have been compared through $t_{1/2}$ recorded during isothermal crystallization experiments at 110 or 120 °C [21]. The relative crystallinity was calculated by integrating for each exotherm the total area under the curve. The $t_{1/2}$ was taken as the time at which the relative crystallinity (area) was equal to 50 %. Table 4 shows the comparative crystallization half-time of PLA nanocomposites containing HNT(QM) and HNT(s).

Table 4 Crystallization half-time ($t_{1/2}$, expressed in minutes) of PLA (processed) and PLA nanocomposites containing HNT(QM) and HNT(s)

Nanofiller, wt % ↓ Crystallization temperature →	HNT(QM)		HNT(s)	
	110 °C	120 °C	110 °C	120 °C
0	6.6	8.8	6.6	8.8
3	3.8	8.3	5.0	8.1
6	7.6	17.4	4.5	6.9
12	7.5	15.2	3.2	5.1

In relation to the addition of HNT(QM), at the exception of the decrease of $t_{1/2}$ specifically recorded for the nanocomposite containing 3 % nanofiller, e.g., at 110 °C from 6.6 to 3.8 min (processed PLA compared to nanocomposite, respectively), the presence of HNT(QM) did not allow for reducing the $t_{1/2}$ values. Noteworthy, these results are supported by the experimental evidence and direct measurements of crystallinity on the specimens obtained by compression molding (the first DSC heating scan, Table 3), the nanocomposite containing 3 % HNT(QM) being characterized by a χ_c of 15.1 %, somewhat higher than those recorded for pristine PLA (10.2 %).

Furthermore, the improved crystallinity of PLA-HNT(s) nanocomposites (Table 3) is in agreement with the determination of $t_{1/2}$ during isothermal crystallization tests at 110 or 120 °C (Table 4) that suggest powerful nucleation ability and higher crystallization kinetics for HNT(s). To explain the higher crystallization (nucleating) effect recorded in presence of HNT(s), several factors should be taken into account such as a better dispersion of nanofiller and more nucleating sites, modification of the interfacial properties by presence of the organomodifier at the nanotube surface. However, it is believed that other techniques, e.g., the polarized optical microscopy (POM) and X-ray diffraction (XRD) can provide additional answers and supplementary information [30].

Morphology and Mechanical Properties

TEM images of PLA-HNT(s) samples at different magnifications reveal that, following the treatment with the silane agent, the dispersion of the nanofiller within PLA matrix appears to be improved (Fig. 8a, b) even at high loadings, i.e., 12 % HNT(s). Overall microscopic analysis indicates well distributed and homogenously dispersed HNT(s) throughout PLA matrix, by considering that the number of clusters/aggregates that can be evidenced in TEM images is lower.

Concerning the mechanical properties, as already specified, on one hand, DMA does not confirm additional improvements using HNT(s) (see Table 2). It is important

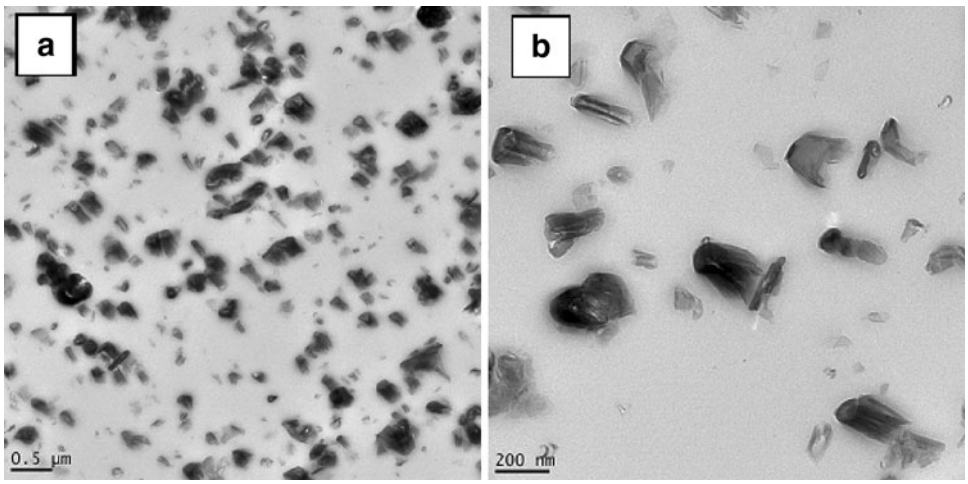

Fig. 8 **a, b** TEM pictures at different magnifications of PLA-12 % HNT(s) nanocomposites

to remind that for these evaluations the possible PLA crystallization during DMA testing, at a relatively low heating rate (3 °C/min), and the differences of crystallinity between the injection-moulded samples were purposely decreased by a previous thermal treatment (at 110 °C, during 90 min, see experimental section).

On the other hand, the values of tensile strength and rigidity are comparable to those obtained using HNT(QM). For instance, it is worth mentioning that addition of 3–6 % HNT(s) yields nanocomposites characterized by a tensile strength of 65 MPa, whereas the modulus of elasticity (2,750 MPa at 6 % HNT(s)) is equivalent to those of PNCs containing HNT(QM). In the same context, it is also important to precise that similarly to HNT(QM), addition of HNT(s) is leading to nanocomposites that do not show the decrease of ε_b, e.g., the ε_b of PLA- 12 % HNT(s) nanocomposite is 6.6 % by comparing to 4.9 %, value obtained for the pristine PLA.

Moreover, as illustrated in Fig. 9, the mechanical testing highlights some improvement for the Izod impact strength (3.5 kJ/m^2 for a nanocomposite containing 12 % HNT(s), only 2.8 kJ/m^2 for pristine PLA), which can be once again connected to the effectiveness of HNT(s). The

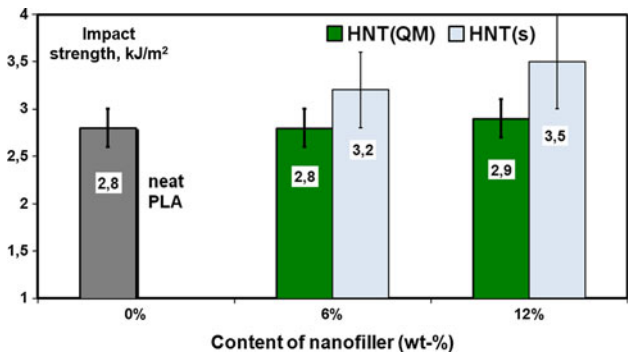

Fig. 9 Impact strength (Izod) of PLA and PLA nanocomposites with different content of HNT(QM) and HNT(s)

enhancement in impact strength is generally ascribed to the fact that the nanotubes play an important role in hindering the cracks induced by impact solicitation or can provoke a bridging, to the absorption of energy by nanotube breakage, to a better interfacial interaction leading to higher absorption of energy during impact deformation and to plastic deformation around nanotubes [25, 27, 31, 49]. In the same context, it is believed that additional factors can explain these improvements: a relatively better dispersion and the decrease of number of agglomerates, assumption which is consistent with TEM investigations, the surface modification and compatibilization with a functionalized silane, without excluding that the crystallization of PLA matrix can play a significant role in toughening as well [50].

Finally, from these results it comes out that addition of HNT(s) is leading to the preservation of PLA thermal stability and evident improvements in the crystallization rate, better impact strength, good rigidity and tensile strength (but not additional increase), correlated to optimistic dispersion through PLA matrix. By comparing to both OMLS and CNT, HNT can represent a good alternative as nanofillers for PLA. Overall testing data suggest that a combination of mechanical strength, rigidity and toughness, associated to a better processing due to a higher speed of crystallization can be obtained by addition of HNT. Furthermore, improvements in melt-mixing (e.g., using twin-screw extruders), compatibilizing and the utilization of co-additives, are expected to lead to nanocomposites with improved properties.

Conclusion

HNT were recently considered as nanofillers for the production of PNCs as possible alternatives to both OMLS and CNT. This first study demonstrates that it is possible to

obtain competitive nanocomposites using HNT and PLA via melt-blending technology. Halloysite, a specific grade (HNT(QM)), has been investigated as potential nanofiller for PLA and the resulting nanocomposites were characterized for highlighting their performances. Following TEM observations, the nanofiller is easily dispersible into PLA matrix, whereas the thermal analyses did not evidence any significant decrease in PLA stability (TGA) or modification of the main thermal parameters (DSC). Their mechanical characterization revealed high tensile strength and Young's modulus (e.g., at 6 % HNT(QM), 70 and 2,800 MPa, respectively), no decrease of ε_b, and good impact properties, at least for a content of (3–12) % nanofiller. As demonstrated by DMA, melt-blending PLA with HNT leads to the enhancement of the storage modulus (E') and offers the possibility to use PLA in applications requiring higher temperature of utilization.

Moreover, the additional nanofiller surface-treatment using 3-methacryloxypropyltrimethoxy silane leads to nanocomposites showing better morphology at higher nanofiller contents, thermal stability and good tensile stress characteristics, associated to higher impact strength (3.5 kJ/m^2 by addition of 12 % HNT(s), with respect to 2.8 kJ/m^2 for pristine PLA). Furthermore, by using HNT(s) the degree of crystallinity (χ_c) of test specimens was found higher, results consistent with the improved PLA nucleating ability and higher rate of crystallization as evidenced by determining the half-crystallization time. By considering the good dispersion into PLA matrix, the panel of mechanical performances due to a significant reinforcing effect of HNT, it is assumed that for targeted uses these nanocomposites may constitute interesting materials for engineering applications.

Acknowledgments Authors thank the Wallonia Region, Nord-Pas de Calais Region and European Community for the financial support in the frame of the IINTERREG IV—NANOLAC project. They thank all partners, especially to Professor Serge Bourbigot (ENSC Lille), Professor Eric Devaux (ENSAIT- Roubaix, France) and their collaborators, for helpful discussions and all mentioned companies for supplying raw materials. This work was also supported by the European Commission and Région Wallonne FEDER program (Materia Nova) and OPTI^{2}MAT program of excellence, by the Interuniversity Attraction Pole program of the Belgian Federal Science Policy Office (PAI 6/27) and by FNRS-FRFC.

References

1. Platt D (2006) Biodegradable polymers—market report. Smithers Rapra Limited UK, Shawbury
2. Drumright RE, Gruber PR, Henton DE (2000) Polylactic acid technology. Adv Mater 12(23):1841–1846
3. Madhavan Nampoothiri K, Nair NR, John RP (2010) An overview of the recent developments in polylactide (PLA) research. Biores Tech 101(22):8493–8501
4. Dubois Ph, Murariu M (2008) The "green" challenge: high performance PLA (nano)composites. JEC Compos Mag 45:66–69
5. Vink ETH, Rábago KR, Glassner DA, Gruber PR (2003) Applications of life cycle assessment to NatureWorks™ polylactide (PLA) production. Polym Degrad Stabil 80(3):403–419
6. Ravenstijn J (2010) The state-of-the-art on bioplastics products: markets, trends, and technologies. Polymedia Publisher GmbH
7. Pluta M (2004) Morphology and properties of polylactide modified by thermal treatment, filling with layered silicates and plasticization. Polymer 45(24):8239–8251
8. Solarski S, Ferreira M, Devaux E, Fontaine G, Bachelet P, Bourbigot S et al (2008) Designing of polylactide/clay nanocomposites for textile applications: effect of processing conditions, spinning and characterization. J Appl Polym Sci 109(2): 841–851
9. Murariu M, Da Silva Ferreira A, Degée Ph, Alexandre M, Dubois Ph (2007) Polylactide compositions. Part 1: effect of filler content and size on mechanical properties of PLA/calcium sulfate composites. Polymer 48(9):2613–2618
10. Bleach NC, Nazhat SN, Tanner KE, Kellomäki M, Törmälä P (2002) Effect of filler content on mechanical and dynamic mechanical properties of particulate biphasic calcium phosphate-polylactide composites. Biomaterials 23(7):1579–1585
11. Murariu M, Bonnaud L, Yoann P, Fontaine G, Bourbigot S, Dubois Ph (2010) New trends in polylactide (PLA)-based materials: "Green" PLA-calcium sulfate (nano)composites tailored with flame retardant properties. Polym Degrad Stabil 95(3):374–381
12. Dubois Ph, Murariu M, Alexandre M, Degée Ph, Bourbigot S, Delobel R, Fontaine G, Devaux E (2008) Polylactide-based compositions. WO patent 095874 Al
13. Murariu M, Da Silva Ferreira A, Duquesne E, Bonnaud L, Dubois Ph (2008) Polylactide (PLA) and highly filled PLA-calcium sulphate composites with improved impact properties. Macromol Symp 272(1):1–12
14. Murariu M, Da Silva Ferreira A, Alexandre M, Dubois Ph (2008) Polylactide (PLA) designed with desired end-use properties: 1. PLA compositions with low molecular weight ester-like plasticizers and related performances. Polym Adv Technol 19(6): 636–646
15. Anderson KS, Schreck KM, Hillmyer MA (2008) Toughening polylactide. Polym Rev 48:85–108
16. Jamshidian M, Tehrany EA, Imran M, Jacquot M, Desobry S (2010) Poly-lactic acid: production, applications, nanocomposites, and release studies. Compr Rev Food Sci Food Saf 9(5):552–571
17. Sinda Ray S, Yamada K, Okamoto M, Ogami A, Ueda K (2003) New polylactide/layered silicate nanocomposites 3 High-performance biodegradable materials. Chem Mater 15(7):1456–1465
18. Fukushima K, Tabuani D, Camino G (2009) Nanocomposites of PLA and PCL based on montmorillonite and sepiolite. Mater Sci Eng C 29(4):1433–1441
19. Villmow T, Potschke P, Pegel S, Haussler L, Kretzschmar B (2008) Influence of twin-screw extrusion conditions on the dispersion of multi-walled carbon nanotubes in a poly(lactic acid) matrix. Polymer 49(16):3500–3509
20. Bourbigot S, Fontaine G, Gallos A, Bellayer S (2011) Reactive extrusion of PLA and of PLA/carbon nanotubes nanocomposite: processing, characterization and flame retardancy. Polym Advan Technol 22(1):30–37
21. Murariu M, Dechief AL, Bonnaud L, Paint Y, Gallos A, Fontaine G, Bourbigot S, Dubois Ph (2010) The production and properties of polylactide composites filled with expanded graphite. Polym Degrad Stabil 95(5):889–900
22. Fukushima K, Murariu M, Camino G, Dubois Ph (2010) Effect of expanded graphite/layered-silicate clay on thermal, mechanical and fire retardant properties of poly(lactic acid). Polym Degrad Stabil 95(6):1063–1076

23. Goffin AL, Duquesne E, Moins S, Alexandre M, Dubois Ph (2007) New organic–inorganic nanohybrids via ring opening polymerization of (di)lactones initiated by functionalized polyhedral oligomeric silsesquioxane. Eur Polym J 43(10):4103–4113
24. Murariu M, Doumbia A, Bonnaud L, Dechief AL, Paint Y, Ferreira M, Campagne C, Devaux E, Dubois Ph (2011) High-performance polylactide/ZnO nanocomposites designed for films and fibers with special end-use properties. Biomacromolecules 12(5):1762–1771
25. Du M, Guo B, Jia D (2010) Newly emerging applications of halloysite nanotubes: a review. Polym Int 59(5):574–582
26. Marney DCO, Russell LJ, Wu DY, Nguyen T, Cramm D, Rigopoulos N, Wright N, Greaves M (2008) The suitability of halloysite nanotubes as a fire retardant for nylon 6. Polym Degrad Stabil 93(10):1971–1978
27. Prashantha K, Schmitt H, Lacrampe MF, Krawczak P (2011) Mechanical behaviour and essential work of fracture of halloysite nanotubes filled polyamide 6 nanocomposites. Compos Sci Technol 71(16):1859–1866
28. Hedicke-Höchstötter K, Lim GT, Altstädt V (2009) Novel polyamide nanocomposites based on silicate nanotubes of the mineral halloysite. Compos Sci Technol 69(3–4):330–334
29. Mingliang D, Baochun G, Demin J (2006) Thermal stability and flame retardant effects of halloysite nanotubes on poly(propylene). Eur Polym J 42(6):1362–1369
30. Liu M, Guo B, Du M, Chen F, Jia D (2009) Halloysite nanotubes as a novel β-nucleating agent for isotactic polypropylene. Polymer 50(13):3022–3030
31. Prashantha K, Lacrampe MF, Krawczak P (2011) Processing and characterization of halloysite nanotubes filled polypropylene nanocomposites based on a masterbatch route: effect of halloysites treatment on structural and mechanical properties. Express Polym Lett 5(4):295–307
32. Zhao M, Liu P (2008) Halloysite nanotubes/Polystyrene (HNT/PS) nanocomposites via in situ bulk polymerization. J Therm Anal Calorim 94(1):103–107
33. Liu M, Guo B, Du M, Cai X, Jia D (2007) Properties of halloysite nanotube-epoxy resin hybrids and the interfacial reactions in the systems. Nanotechnology 18(45):455703
34. Deng S, Zhang J, Ye L (2009) Halloysite–epoxy nanocomposites with improved particle dispersion through ball mill homogenisation and chemical treatments. Compos Sci Technol 69(14):2497–2505
35. Fleischer C, Daly R, Wagner A, Kelley D, Duffy M (September 17, 2008) Clay nanotubes in polymer composites: a route to stronger, lighter & less expensive materials. In: 8th annual SPE automotive composites conference & exhibition, Michigan
36. Cooper S, Fleischer C, Michael D, Aaron W (2011) Polymeric composite including nanoparticle filler. United States Patent 2011/0160345 A1
37. Cooper S, Fleischer C, Michael D, Aaron W (2011) Polymeric composite including nanoparticle filler, United States Patent 7,888,419 B2
38. ***HNT^{TM}-QM, MSDS—material safety data sheet 0023, August 6, 2007
39. Sadler EJ, Vecere AC (1995) Silane treatment of mineral fillers-practical aspects. Plast Rub Compos Pro 24(5):271–275
40. Cervantes-Uc JM, Cauich-Rodriguez JV, Vazquez-Torres H, Garfias-Mesias LF, Paul DR (2007) Thermal degradation of commercially available organoclays studied by TGA-FTIR. Thermochim Acta 457(1–2):92–102
41. Quantin P, Herbillon AJ, Janot C, Siefferman G (1984) L'halloysite blanche riche en fer de vate (Vanuatu). Hypothese d'un edifice interstratifié halloysite-hisingerite. Clay Miner 19: 629–643
42. Yuan P, Southon PD, Liu Z, Green ME, Hook J, Antill SJ, Kepert CJ (2008) Functionalization of halloysite clay nanotubes by grafting with gamma-aminopropyltriethoxysilane. J Phys Chem C Nanomater Interfaces 112(40):15742–15751
43. ***Guide to Silane Solutions from Dow Corning. (Dow Corning Corporation, 2005) http://www.talleresnorte.com.ar/pdf/pinturas/silanos/silane_guide.pdf
44. Lecouvet B, Gutierrez JG, Sclavons M, Bailly C (2011) Structure property relationships in polyamide 12/halloysite. Polym Degrad Stabil 96(2):226–235
45. Yasuniwa M, Tsubakihara S, Sugimoto Y, Nakafuku C (2004) Thermal analysis of the double-melting behavior of poly(L-lactic acid). J Polym Sci Part B Polym Phys 42(1):25–32
46. Su Z, Li Q, Liu Y, Hu G-H, Wu C (2009) Multiple melting behavior of poly(lactic acid) filled with modified carbon black. J Polym Sci Part B Polym Phys 47(20):1971–1980
47. Pluta M, Murariu M, Alexandre M, Galeski A, Dubois P (2008) Polylactide compositions The influence of ageing on the structure, thermal and viscoelastic properties of PLA/calcium sulfate composites. Polym Degrad Stabil 93(5):925–931
48. Handge UA, Hedicke-Höchstötter K, Altstädt V (2010) Composites of polyamide 6 and silicate nanotubes of the mineral halloysite: influence of molecular weight on thermal, mechanical and rheological properties. Polymer 51(12):2690–2699
49. Deng S, Zhang J, Ye L, Wu J (2008) Toughening epoxies with halloysite nanotubes. Polymer 49(23):5119–5127
50. Oyama HT (2009) Super-tough poly(lactic acid) materials: reactive blending with ethylene copolymer. Polymer 50(3):747–751